Device Parameter Optimization of Silicon Germanium HBT for THz Applications

Pradeep Kumar and R. K. Chauhan

Department of ECE, M.M.M. Engineering College
Gorakhpur-273010
pradeep.hitesh@gmail.com
rkchauhan27@gmail.com

Abstract: Now-a-days SiGe HBTs are surpassing even the fastest III-V production devices in the high–speed orbit. The state-of-art in simulation of silicon germanium semiconductor devices is presented in this paper. A comprehensive course of action to model the device parameter characterization of High Frequency 0.1μm SiGe HBT is depicted which is based on the technique of direct parameter extraction. With the help of S-, Y- and Z- parameters, the equivalent circuit parameters have been extracted in a faultless approach. The intrinsic and the extrinsic elements of model are obtained using a direct extraction method that assists to find out the base resistance from the Z- parameters. In this, the issues entailed in simultaneous optimization of f_{max} and f_T and related optimization of base resistance as well as junction capacitance are addressed. The device characteristics of the SiGe HBT are found much advance to those of III–V semiconductor devices. A corroboration of objective validity of the modeling scheme and the extraction of parameter is accomplished in the form of S-parameters. These results have been validated using a viable numerical device simulator ATLAS from Silvaco International.

Keywords: Si, Ge grading, SiGe HBT, cut-off frequency, f_{max} , MSG.

1. Introduction

The silicon bipolar technologies were attaining development with delays in ECL gate between 20 and 30 ps as well as cut-off frequency f_T about 30GHz in late 80s. Further, there were noteworthy developments when Silicon-Germanium Heterojunction bipolar transistor (HBT) emerged from research laboratories in viable world and entered fabrication in conventional radio frequency BiCMOS technologies in the 90s. Due to such developments, a impressive impact on the performance on bipolar transistors was noticed which in turn caused f_T values approaching 400GHz and values of ECL gate delays less than 5 ps. In addition, SiGe BiCMOS technology is sincerely challenging III/V and II/VI technologies in realm of high-frequency electronics applications, for example optical fibre and mobile communications. Also, the way for employing SiGe in CMOS technologies have been cemented by these successes of SiGe in bipolar technologies.

Since SiGe is used to furnish improved channel mobility in a number of different types of Heterojunction MOSFET, an akin revolution is now in progress in the fabrication of MOS transistors. 0.13 mm CMOS device technology in present is soundly compatible with the devices. The viability of consciousness of a complete wireless system on-a-chip is presented by this compatibility. The emergence of Silicon Germanium BiCMOS technology by combining $Si_{1-x}Ge_x$ HBT circuits with digital application-specific integrated circuits (ASICs) is currently in highly production. From Ammar & R.K.Chauhan model, it is suggested that the current gain of the SiGe HBT can be tailored effectively for high speed applications and it is also inferred that such HBTs have greater flexibility in the design compared to BJTs as one can easily reduce the base resistance without losing much of the gain [1]. Upcoming generation of 40, 80,

Received: August 13, 2010. Accepted: December 27, 2010

or 100 Gb/s communications channels will be operated, due to complete improvement of optical-fiber trunk lines in comparison with the current 2.5-10 Gb/s communications channels. It is estimated that manufacture of 100 Gb/s links might be pace since 2010-2011.

In this paper, we explored the upshot of Ge grading on the performance of $Si_{1-x}Ge_x$ HBT. The extrapolated maximum oscillation-frequency f_{max} , cutoff frequency f_T, stability, Figure-of merit, power gain and various intrinsic as well as extrinsic parameters are calculated for different Ge concentrations with linear grading. Following this motivation, in second section, we address model of $Si_{1-x}Ge_x$ HBT and its elements. In Section-III, we discuss the high frequency characterization. In the fourth Section, we address the HF modeling and performance factors of this SiGe HBT with the help of small-signal analysis as well as in fifth section, we discuss the results based on ATLAS. Finally, in section sixth, we concluded with common projections and observations.

2. Model

The energy-band diagram of resultant device is the paramount mean to portray a range of consequences of introducing Ge into the base region of SiGe HBT by comparing it to Si. The graded base induces a drift field across the neutral base that is aligned in a direction (from collector to emitter). This causes an acceleration of induced minority electrons across the base. Consequently, this large drift field component is a domino effect for electron transport phenomenon. Hence, by effectively speeding up the diffusive transport of the minority carriers a decrement in the base transit time occurs. Although the band offsets in SiGe HBTs are usually small in comparison to the band offsets of III-V technology standards, the large electric fields are translated by the Ge grading over the short distance of neutral base and this electric field is ample to speed up the electrons to near saturation velocity. In comparison to SiGe HBT, the base transit time typically limits the frequency response of the Si BJT. Therefore it could be predictable that the frequency response should be improved appreciably by the Ge- induced drift field [2]. The cross-section of the SiGe HBT base is shown in Figure (1.b).The bandgap of SiGe HBT is given by [3],

$$E_g^{SiGe} = E_g^{Si} \cdot (1-x) + E_g^{Ge} \cdot x + C_g \cdot (1-x) \cdot x \tag{1}$$

Where x is Ge conc. and C_g = -0.4 eV is a bowing parameter. Ge is compositionally graded from the emitter-base (EB) junction with lower concentration to the collector–base (CB) junction with higher concentration and it is shown as dashed line in Figure (1.a). Due to this impact, the SiGe HBT consists of a finite band offset at the EB junction and a larger band offset at the CB junction. Bandgap grading is easily used for position dependence of the band offset with respect to Si. An electric field is produced by such position dependence in the Ge induced band offset in the neutral base region. This effect aids the transportation of minority carriers (electrons) from emitter to collector, which in turn improve the frequency response [4-6], [7-1].

Thus we can say apparently from Figure (1.a) that the Ge-induced reduction in base bandgap takes place at the EB edge of the quasi-neutral base $\Delta E_{g,Ge}$ (x=0) along with the CB edge of the quasi-neutral base $\Delta E_{g,Ge}$ ($x=W_b$). Thus the graded bandgap is given by equation as [8],

$$\Delta E_{g.Ge}(grade) = \Delta E_{g.Ge}(W_b) - \Delta E_{g.Ge}(0) \tag{2}$$

Such Ge grading across the neutral base induces a built-in-quasi drift field ξ.

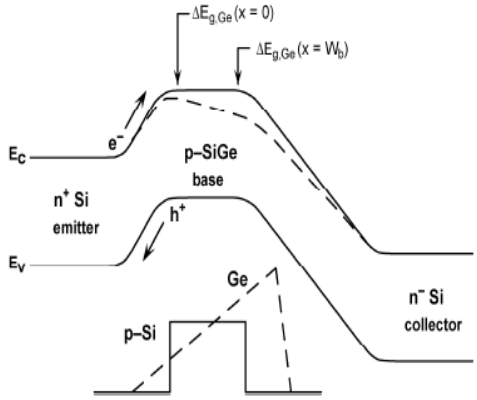

Figure 1a. Energy band diagram for a Si BJT and graded-base SiGe HBT, both biased in forward active mode at low injection

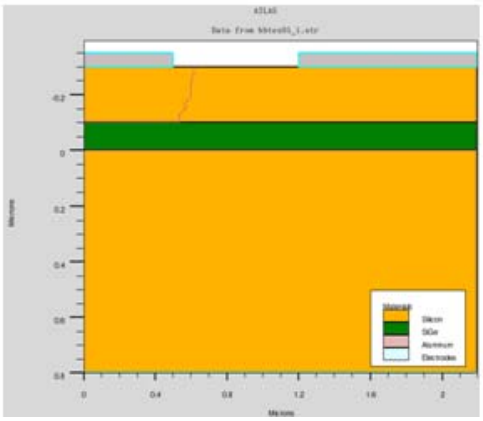

Figure 1b. The cross-section of Sige HBT

For instance, compared to a comparably designed Si BJT, the Ge-induced band offsets in a SiGe HBT exponetially counteracts the the bandgap narrowing of the emitter to produce a current-gain as [2],

$$\frac{\beta_{SiGe}}{\beta_{Si}} = \gamma\eta \frac{\Delta E_{g.Ge(grade)} \Big/ kTe^{\Delta E_{g.Ge(0)}/kT}}{1 - e^{-\Delta E_{g.Ge(grade)}/kT}} \tag{3}$$

The base transit time of SiGe HBT is compared to the base transit time of Si transistor as [8],

$$\frac{\tau_{B,SiGe}}{\tau_{B,Si}} = \frac{2}{\eta} \cdot \frac{kT}{\Delta E_{g,}Ge(grade)} \cdot \left\{1 - \frac{kT}{\Delta E_{g,Ge}(grade)}\left[1 - e^{-\Delta E_{g,Ge(grade)}/kT}\right]\right\} \tag{4}$$

And η is the electron diffusivity ratio between SiGe and Si as [8],

$$\eta = \frac{(D_{nb})SiGe}{(D_{nb})_{Si}} \tag{5}$$

And an “effective density-of-states ratio” between SiGe and Si according to

$$\gamma = \frac{(N_c N_v)_{SiGe}}{(N_c N_v)_{Si}} < 1 \tag{6}$$

Thus built-in field increases on decreasing the base width so the transit time decreases on higher built-in field ξ and higher collector current I_c. Here W_B is the width of the quasi-neutral base; D_{nb} is the diffusion coefficient of the minority- carrier electrons in the base. The cut-off frequency f_T can be calculated from the following expression of the Total emitter-collector delay time as [11],

$$1/2\pi f_T = \tau_B + \tau_c + \frac{\eta k T}{q I_c}(C_{BE} + C_{BC}) + (R_E + R_c) C_{BC} \quad (7)$$

It is understandable that the cut-off frequency inversely depend on the base transit time τ_B. So higher cut-off frequency devices need the smaller value of the transit time. The maximum oscillation frequency f_{max} is calculated from f_T as [2],

$$f_{max} = \sqrt{\frac{f_T}{8\pi C_{CB} R_B}} \quad (8)$$

Where C_{BC} is the base-collector junction capacitance and RB is the base resistance. Thus from equation (8) it is comprehensible that lower base-collector junction capacitance and base resistance are required for the higher value of f_{max} . So the cut-off frequency f_T is increases as transit time decreases which in turn affect the f_{max} [3-8].

3. High Frequency (THz) Characterization

High frequency devices are characterized by several methods. These methods include the scattering parameter(S-parameter) measurement by means of a network analyzer. S-parameter measurement is a mean of a small signal measurement. The main issue in this measurement is the calibration with accurately de-embedding the parasitic. The load-pull measurement, a very useful technique is used for power measurements, even though it is costly and time consuming. A set of two-port parameters [including Z-, Y-, H-, ABCD-, and S- parameters] are used to describe the small signal RF performance of SiGe HBT. One type of parameters can simply be converted into another type of parameters with the help of matrix manipulation. The Y-parameters are frequently most suitable for equivalent circuit based analysis whereas the s-parameters are almost absolutely used for RF as well as microwave measurements due to practical reasons [12].

A. S-parameters:

The device under test (DUT) often oscillates by open and short terminations because at very high frequencies, accurate open and short circuits are not easy to attain due to inherent parasitic capacitances and inductances. The interconnection between the DUT and test apparatus is also akin to the wavelength. The consideration of distributive effects is required in this case. So S-parameters were developed and are almost absolutely used to portray transistor RF with Microwave performance due to these practical difficulties.

S-parameters have almost similar information like Z-, Y-, or H-parameters. But the difference between them is that the dependent and independent variables are no longer simple voltages and the currents in S-parameters. In addition, in the s-parameter four “voltage waves” are produced by linear combinations of the simple variables. These voltage waves hold the identical information because they are chosen to be linearly independent. Transmission line techniques are used to compute s-parameters at high frequencies by properly selection of these combinations.

If incident wave is indicated by ‘a’ and reflection or scattering is indicated by ‘b’. Here the voltage waves are defined using voltages and currents for characteristic impedance Z_0. Thus

voltages (a_1, a_2) are called incident waves, while (b_1, b_2) are called scattered waves. A set of linear equations is used to relate the scattered waves with the incident waves by just as the port voltages are related to the port currents by Z-parameters.

It is expressed like,

$$\begin{pmatrix} b_1 \\ b_2 \end{pmatrix} = \begin{pmatrix} S_{11} & S_{12} \\ S_{21} & S_{22} \end{pmatrix} \begin{pmatrix} a_1 \\ a_2 \end{pmatrix} \tag{9}$$

Where,

S_{11} is simply reflection coefficient corresponding to input impedance with Z_0 output termination.

S_{22} is output reflection coefficient looking back into the output for Z_0 source termination.

$|S_{21}|^2$ is transducer gain for a Z_0 source and Z_0 load.

$|S_{12}|^2$ is reverse transducer gain for a Z_0 source and a Z_0 load. Thus S-parameters of a SiGe HBT will thoroughly depend on the size of transistor, frequency of operation as well as on biasing condition.

B. De-Embedding:

De-Embedding is the process for removing; de-embed (the surrounding parasitic). This is done for characterizing only intrinsic part of the device. There are numerous ways to de-embed the parasitic with diverse levels of precision and complication. The first simple and directly way is to apply lumped circuit model for representing the parasitic. Secondly, compose device under test with different width by using identical metal pattern. When it is done then admittance is used to estimate the parasitic. This admittance is achieved when the width is extrapolated to zero. Furthermore, relate the similar calibrations routines and these routines are built-in VNA. Thus De-Embedding process can be completed by two ways; initially by using the calibration structures during calibrating the network analyzer and secondly by calibration on standard ISS (impedance standard substrate).

4. HF Modeling and Performance Factors

In this section we develop a novel and uncomplicated extraction method for discussing the transistor RF performance along with procedures to find out the parameters of SiGe HBT by means of small-signal Π topology equivalent circuits of this HBT. The algorithm is helpful for extracting both intrinsic plus extrinsic (parasitic) elements. If we determine formerly the extrinsic elements of the HBT then conventional procedures or methods derived from simple bias measurements work very sound. Through different procedures for example DC, cut-off measurements, or optimization can be used for this approach. Since the typical DC and cut-off techniques present poor performance for Silicon Germanium HBT devices that's why it is frequently very hard to precisely determine the values of parasitic elements of the HBT. An innovative technique has been developed to circumvent this problem and in this technique only scattering (S)-parameters at different biases are measured. For fitting the measured S-parameters appropriately, linear models by way of a Π topology have been experienced. We have neglected emitter resistance, the collector resistance, along with the output resistance due to Early effect for simplicity [13].

S-parameters obtained from ac analysis are simply converted into Y-, Z- or H-parameters using ATLAS. Various Power Gains for example MAG (maximum available gain), MSG (maximum stable gain) as well as MAUG (maximum available unilateral gain) are used for analysis. Furthermore, a Figure-of-merit that has been used extensively for microwave

characterization is MSG. Due to simplicity of measurement at high frequencies these quantities are calculated from the measured small-signal scattering parameters.

The maximum stable gain is calculated by y_{21} and y_{12} as,

$$MSG = \left| \frac{y_{21}}{y_{12}} \right| \tag{10}$$

And the maximum available gain is extracted as,

$$MAG = \left| \frac{y_{21}}{y_{12}} \right| \left(k - \sqrt{k^2 - 1} \right) \tag{11}$$

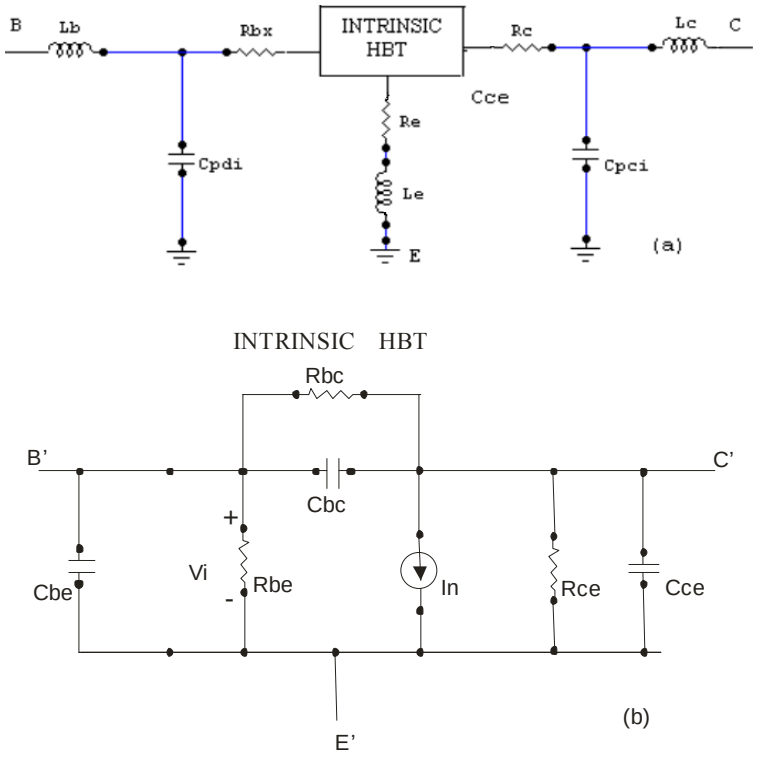

Figure 2 A small-signal Π equivalent circuit of an HBT device (a) contains intrinsic and extrinsic circuit elements. The intrinsic elements (b) can be determined from the admittance parameters of the device at a number of different bias points.

Where *k* is *'Rollett stability factor'* and extracted by this equation as,

$$k = \frac{2\,\mathrm{Re}(y_{11})\,\mathrm{Re}(y_{22}) - \mathrm{Re}(y_{12}\,y_{21})}{|y_{12}\,y_{21}|} \tag{12}$$

Mansion's gain is obtained by the following equation as,

$$U = \frac{\left|y_{21} - y_{21}\right|^2}{4\left[\mathrm{Re}(y_{11})\,\mathrm{Re}(y_{22}) - \mathrm{Re}(y_{12})\,\mathrm{Re}(y_{21})\right]} \tag{13}$$

The maximum available unilateral gain is calculated by this equation as,

$$MAUG = \frac{\left|y_{21}\right|^2}{4\,\mathrm{Re}(y_{11})\,\mathrm{Re}(y_{22})} \tag{14}$$

When both input and output are concurrently conjugate matched, at this state we achieve MAG. When k > 1, at this the device is unconditionally stable and MAG exists. It is obvious from equations (13) and (14), if the device is unilateral (y_{12} = 0) then U equals to MAUG. When the device is unconditionally stable then MAG equals to MSG and vice-versa. Maximum frequency at which MSG becomes unity is frequently termed as f_{max}. As power gain with no impedance transformation is achieved by common-emitter microwave transistors. This is the reason why these transistors may comprise useful gain when inserted into a system with 50 Ω.

For this model, MSG (maximum stable gain) is called FOM (Figure of merit). This device is unconditionally stable here.

f_T does not consider the limitations due to physical base resistance RB but it is usually used to depict the frequency response of a bipolar transistor. Moreover another parameter named maximum oscillation frequency f_{max} includes the effect of RB, with the parameters in f_T . The maximum oscillation frequency f_{max} is the extrapolated frequency at which the small signal power gain is reduced to unity when the terminations are conjugatly matched at both input and output. From the extrapolation of the high-frequency asymptote of a plot of the magnitude of h_{21} in dB versus log (frequency), we can extract the unity gain cut-off frequency. At amply low frequency most bipolar transistor devices may be depicted as single pole devices. This theory is alike to a high-frequency asymptote with a slope of −20 dB per decade so is the cut-off frequency though both C_{BE} and C_{BC} capacitances are bias dependent. f_{max} is extracted at the point where MSG becomes 0 dB from MSG (in dB) versus log (frequency) plot [14-15].

We can achieve the intrinsic elements from the admittance parameters of the HBT device for each bias point after a usual de-embedding process for taking the consequence of parasitic elements. The intrinsic elements for example C_{BE} (base-emitter capacitance) vary with frequency. The intrinsic part of the device (Figure 2b) is contained by the given circuit topology of the small-signal model which is shown by dashed box in Figure (2a). For a number of different devices tested, the estimated values of the pad parasitic capacitances C_{pbi} along with C_{pci} do not surpass hundredths of femto Farads (fF) due to this fact these capacitances can be omitted. The intrinsic and extrinsic parameters in Figure 2 can be extracted by the following method [16]:

The base-emitter junction capacitance is calculated by the equation as follow [16],

$$C_{BE} = \frac{I_m[y_{11}] + I_m[y_{12}]}{\omega_i} \tag{15}$$

The base-collector junction capacitance is expressed by the equation as follow [16],

$$C_{BC} = \frac{-I_m[y_{12}]}{\omega_i} \tag{16}$$

The base-collector junction capacitance is expressed by the equation as follow [16],

$$C_{CE} = \frac{I_m[y_{22}] + I_m[y_{12}]}{\omega_i} \tag{17}$$

The base-collector junction capacitance is calculated by the equation as follow [16],

$$R_{BC} = \frac{-1}{\mathrm{Re}[Y_{12}]} \tag{18}$$

The collector-emitter junction resistance is obtained by the equation as follow [16],

$$R_{CE} = \frac{1}{\mathrm{Re}[Y_{12}] + \mathrm{Re}[Y_{22}]} \tag{19}$$

The collector-emitter junction resistance is expressed by the equation as follow [16],

$$R_{BE} = \frac{1}{\mathrm{Re}[Y_{11}] + \mathrm{Re}[Y_{12}]} \tag{20}$$

And extrinsic resistance is obtained by the equation as follow [16],

$$R_{EXTRINSIC} = Z_{11} - Z_{12} \tag{21}$$

In this method C_{BE} are intrinsic junction capacitances and $R_{BC,}$ R_{CE} and R_{BE} are intrinsic junction resistances.

5. Results and Discussion

Based on the above model the values of f_{max} / f_T and various intrinsic as well as extrinsic elements are calculated for n-p-n SiGe HBT at different Ge concentrations for linearly graded Ge. For this purpose ATLAS from SILVACO International is used. The HBT considered in this paper has the base width of 0.1μm. Average Ge concentration in this base region considered in our calculations is varied from 8%-25% as higher to this are not supported by present epitaxial technologies and beyond it the improvement associated with Ge seizes may be due to lattice constant mismatch as in Figure 6. ATLAS simulation of SiGe HBT is performed to prove precision.

With the intention of getting excellent accord with measured characteristics, all the important physical effects, for example impact ionization (II) is appropriately modeled and accounted for the simulation as well. The impact ionization leads to a strong enhancement of Ic. AC simulation needs apposite DC calibration which is an important prerequisite for it. For this simulation, it is compulsory to take the complete device composition into account with the aim of considering the capacitance between substrate and collector (C_{CS}) as well as capacitance between base and collector (C_{BC}). Figure 3.1 to Figure 3.3 show the simulated S-parameters at V_{CE} = 1V for this device. Because of the intuitive relationship between coefficients S_{11} and S_{22} are conveniently on a smith chart, while S_{21} and S_{12} are representing the gain response that's why they are typically displayed on a polar plot. The methods other than the method of polar plot are not convenient to represent the gain like Figure 7 'mod of S_{12} (dB) and mod of S_{21} (dB) vs. frequency plot' (bode plot). In the Figure 3.1 to 3.3, the S_{11} for a bipolar transistor always moves clockwise as frequency increases on the smith chart. The S_{11} data at higher I_C in general shows a smaller negative reactance, because of the higher EB diffusion capacitance.

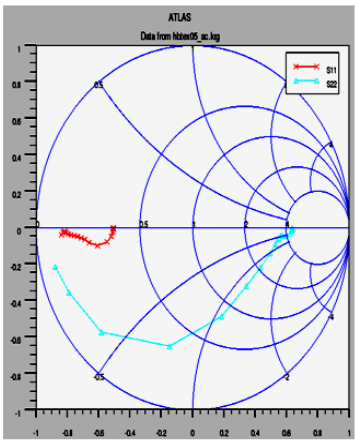

Figure 3.1. Simulated S11 and S22 Parameters from ATLAS at 0.25 Ge concentrations

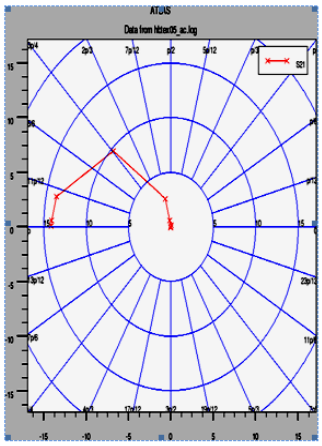

Figure 3.2. Simulated S21 parameter Parameter from ATLAS at 0.25 Ge concentrations

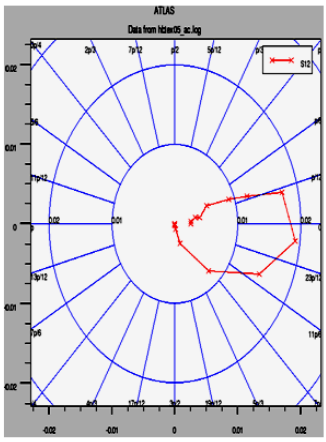

Figure 3.3. Simulated S12 parameter Parameter from ATLAS at 0.25 Ge concentrations

current. It follows from the above discussion that the S-parameters of a SiGe HBT will intimately depend on the transistor size, biasing condition and operating frequency [17]. Using ATLAS and above HF model the extrapolated f_{max} is calculated 16.8 THz and f_T is calculated 13.5 THz for 0.25 Ge concentration. Figure 5 shows the power gain MSG (dB) vs. frequency (Hz). At 8.19 GHz frequency Figure-of-merit MSG at 0.25 Ge concentration is calculated 31.54 dB.

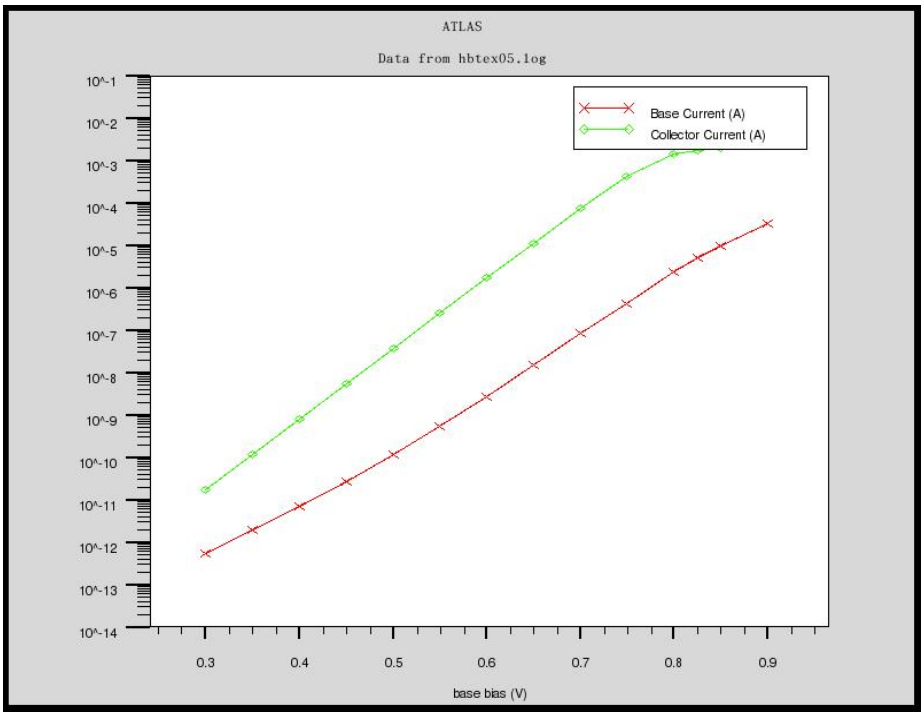

Figure 4. Gummel plot of SiGe HBT as a function of EB voltage for an SiGe HBT

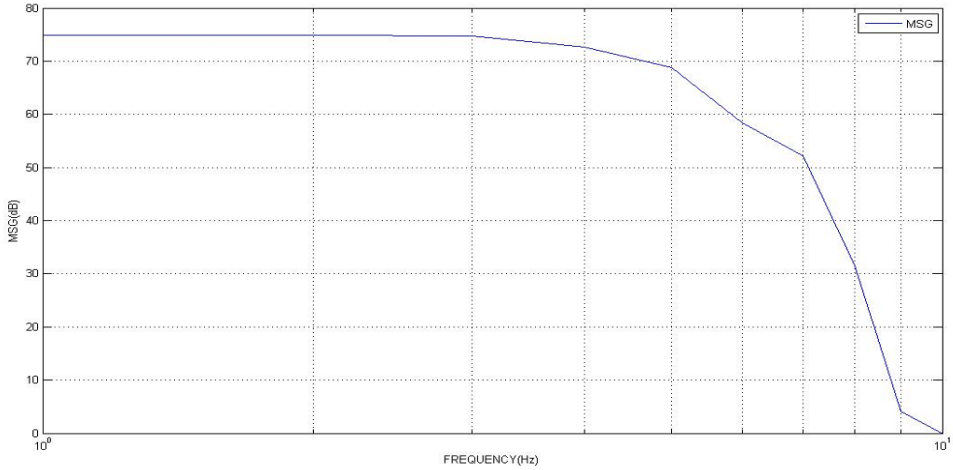

Figure 5. MSG (dB) vs. frequency (Hz) plot at 0.25 Ge conc.

The Gummel plot for this model at 1V forward bias is plotted in Figure 4. The plot in Figure 4 shows the variation of collector current and base current w.r.t. bias voltage. This plot indicates to the important dc consequence of adding Ge into the base, however, lies with the collector current density [2]. Physically, the barrier to electron injection at the EB junction is reduced by introducing Ge into the base, yielding more charge transport from emitter-to-collector for a given applied EB bias. Observe from Figure (1.a) that in this linearly graded-base design, the emitter region of the SiGe HBT and Si BJT comparison are essentially identical, implying that the resultant base current density of the two transistors will be roughly the same. The net result is that the introduction of Ge increases the current gain of the transistor (β=collector current density / base current density). From a more device–physics oriented viewpoint, the Ge-induced band offset exponentially decreases the intrinsic carrier density in the base which, in turn, decreases the base Gummel number and, hence, increases collector current density. Meaningful in this context is the Ge-induced improvement in β over a comparably constructed Si BJT [2].

The intrinsic and the extrinsic parameters are calculated for the above model of SiGe HBT. The values of these parameters are in the Table.1.

Table.1 Summary of Device parameters from2D simulation

Ge conc.	f_{max} (THz)	R_B(Ω.μm)	C_{BC}(f F)	C_{BE}(f F)	C_{CE}(f F)
0.2	8.39	5.71	72	44.33	54.7
0.25	16.8	4.251	66	27.9	52.45

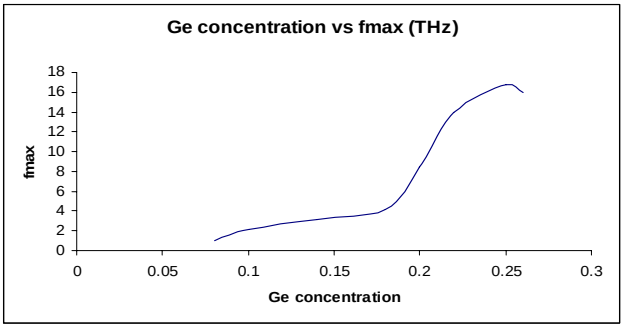

Figure 6. Plot of f_{max} (THz) vs. Ge concentration

Now we will discuss some practical issues of employing the base region optimization approach. This device results in the lower power consumption which can be used for battery operated low cost devices for high speed applications. Now-a-days research shows that applications in high-frequency communications and radar employ the wide bandwidth heterojunction bipolar transistors (HBTs). ICs for 40 Gb/s transmission are currently in development in optical fiber communications. Ample improvements in the bandwidth of semiconductor electronics indicate that this improved bandwidth will be utilized by the emerging 160 Gb/s transmission equipment in the vicinity of future. Thus it can be proposed that devices with THz frequency are used for dust and line as well as continuant radiation from cool (5-100 K) gas (molecules and atoms).

This HBT in Tera-Hertz frequencies encompass definite water absorption rates and imitate off metal, except this it can usually infiltrate fog and fabrics [18]. Chemical detection, medicine, chemical spectroscopy, transportation and national security in addition with weapon fields will also be enriched with this HBT. The study of Dust & gas chemistry, stellar and galactic constituents as well as evolution cosmology will be helped by these THz devices. This HBT in THz Radar will accommodate in investigating hidden universe and planet.

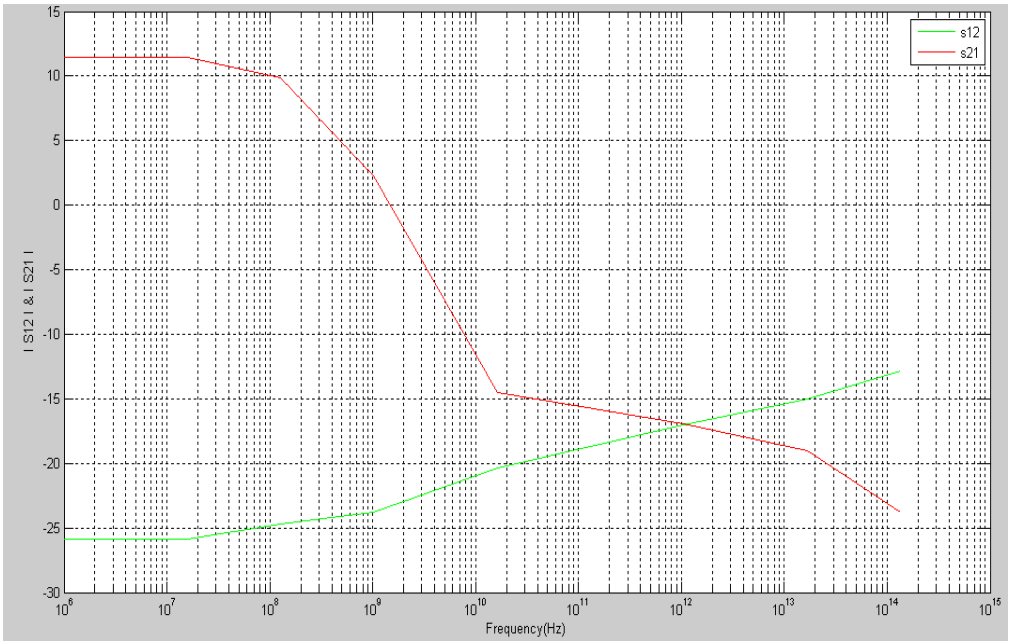

Figure 7. Mod S_{12}(dB) and mod S_{21}(dB) vs. Frequency plot (Hz)

Conclusion

In this paper, a detailed investigation has been made to study the impact of Ge content and Ge grading in the SiGe-HBT base on the performance of the HBT. An electric field is produced by position dependence in the Ge induced band offset in the neutral base region. This effect aids the transportation of minority carriers (electrons) from emitter to collector, which in turn improve the frequency response. High frequency devices are characterized by extracted s-parameters. S-parameters are measured by means of a small signal measurement. In this paper, we develop a novel and uncomplicated extraction method for discussing the transistor RF performance along with procedures to find out the parameters of SiGe HBT by means of small-signal Π topology equivalent circuits of this HBT. S-parameters obtained from ac analysis are

simply converted into Y-, Z- or H-parameters using ATLAS. Further the intrinsic and extrinsic parameters which affect the f_{max}/f_T are calculated. The base-region optimizations can effectively improve the power-gain values of $Si_{1-x}Ge_x$ HBTs in a wide frequency range. In this model, the power gain MSG produces the THz f_{max}/f_T which is very fruitful for the tera Hz applications. The extrapolated f_{max} using ATLAS is calculated 16.8 THz and f_T are calculated 13.5 THz for 0.25 Ge concentration. At 8.19 GHz frequency MSG at 0.25 Ge concentration is calculated 31.54 dB. Low base resistance for SiGe power HBTs are realized by the appositely optimized base-region with a high Ge content of appropriate form. This model is also used to realize microwave power amplification at high frequencies using these devices has been verified to be viable.

References

[1] Vishal, Ammar and R.K. Chauhan. "Performance Analysis of a Bandgap Engineered Silicon Bipolar Transistor", *Proc of International Conference "ELECTRO-2009", IT BHU*, Dec. 22-24, (2009).

[2] J. D. Cressler. SiGe HBT technology: "a new contender for Si-based RF and microwave circuit applications". *IEEE Trans. Microw. Theory Tech*., vol. 46, issue 5, 572 (1998).

[3] V. Palankovski and S. Selberherr. "Critical modeling issues of SiGe semiconductor devices", *J. Telecommun. Inform. Technol*., no. 1, 15 (2004).

[4] Ankit Kashyap and R. K. Chauhan. "Profile Design optimization of SiGe based HBT for High Speed Applications", *Journal of Computational and Theoretical Nanosciences,* Vol. 5, 2238, (2008).

[5] Ankit Kashyap and R. K. Chauhan. "Effect of the Ge profile design on the performance of an n-p-n SiGe HBT-based analog circuit", *Microelectronics journal, MEJ*: 2554, (2008).

[6] Mukul K Das, N. R. Das and P. K. Basu. "Performance Analysis of a SiGe/Si Heterojunction Bipolar Transistor for Different Ge-composition", *Proc. of the International Conf. URSI-GA, New Delhi*, D03.7 (2005).

[7] Ankit Kashyap, Ashok Kumar and R. K. Chauhan. "Design of a High Speed SiGe HBT for Wireless Applications", *Proc. of International Conference IICT-2007, DIT, Dehradoon* July 27-28 (2007).

[8] John D. Cressler. "Emerging SiGe HBT Reliability Issues for Mixed-Signal Circuit Applications", *IEEE Transactions on Device and Materials Reliability*, vol. 4, no. 2 (2004).

[9] Richard S. Muller, Kamins and Mansun Chan. "Device Electronics for Integrated Circuits", *3rd ed., Jhon Wiley & Sons Publication* (2002).

[10] Peter Ashburn. "SiGe Hetrojunction Bipolar Transistors", *Jhon Wiley & Sons Publication* (2003).

[11] Ping-Chun Yeh, Chih-Hung Hsieh, Chwan-Ying Lee, Yu-Lin Chu, Kuan-Lun Chang, Denny Tang , John Chern and Hwann-Kaeo Chiou. "Geometrical Effect Analysis on f_T and f_{max} of 0.18 μm SiGe HBT", *Microwave and RF Laboratory, PAWorkshop, National Central University* (2004).

[12] Lars Vestling. "Design and Modeling of High-Frequency LDMOS Transistors", 681, ACTA. Universitatis UPSALIENSIS UPPSALA (2002).

[13] ATLAS User's Manual DEVICE SIMULATION SOFTWARE, SILVACO International, (2004).

[14] Zhenqiang Ma, Saeed Mohammadi, Pallab Bhattacharya, Linda P. B. Katehi, Samuel A. Alterovitz, George E. Ponchak. "A High-Power and High-Gain X-Band Si/SiGe/Si Heterojunction Bipolar Transistor", *IEEE Transactions on Microwave Theory and Techniques*, vol. 50, No. 4, April (2002).

[15] Zhenqiang Ma and Ningyue Jiang. "Base–Region Optimization of SiGe HBTs for High-Frequency Microwave Power Amplification", *IEEE Transactions on Electron Devices*, vol. 53, No.4, April (2006).
[16] J. M. Zamanillo, A. Tazon, A. Mediavilla and C. Navarro. "Simple Algorithm Extracts SiGe HBT Parameters", MICROWAVES & RF (1999).
[17] Application note 154 on S-Parameter Design, Hewlett-Packard (1990).
[18] Frank Chang. "Terahertz CMOS SoC for Imaging/Communication Systems", UCLA, High-Speed Electronics Laboratory.

Pradeep Kumar was born in Allahabad, India in 1985. He received his B.Tech. degree in Electronics & Communication Engineering in 2006. He initially joined VINCENTIT Hyderabad in 2006 and thereafter worked as a lecturer in Dr. K.N.M.I.E.T. Modinagar, Ghaziabad between 2007 and 2008. He is currently pursuing the M.Tech. degree in Digital Systems from Madan Mohan Malviya Engineering College, Gorakhpur, India. His M.Tech. thesis is dedicated towards the modeling and device parameter optimization of Silicon-Germanium HBT for THz applications.

e-mail: pradeep.hitesh@gmail.com
Ph: +91-9453291241
Deparment of ECE, Madan Mohan Malviya Engineering College, Gorakhpur-273010, India.

R. K. Chauhan was born in Dehradoon, India in 1967. He received the B.Tech. degree in Electronics & Communication Engineering, from G.B.P.U.A.T - Pantnagar, in 1989 and M.E. in Control & Instrumentation, from MNNIT-Allahabad in 1993 and Ph.D in Electronics Engineering, from IT-BHU, Varanasi, INDIA in 2002. He joined the department of ECE, Madan Mohan Malviya Engineering College, Gorakhpur, India as a lecturer, in 1993, as an Assistant Professor since 2002 and thereafter as an Associate Professor since Jan, 2006 to till date in the same institute. He also worked as a Professor in Department of ECE, Faculty of Technology, Addis Ababa University, Ethiopia between 2003 to 2005. He is reviewer of Microelectronics Journal, CSP etc.. His research interests include device modeling and simulation of MOS, CMOS and HBT based circuits. He was selected as one of top 100 Engineers of 2010 by International Biographical Centre, Cambridge, England.

e-mail: rkchauhan27@gmail.com
Ph: +91-9235500556
Department of ECE, Madan Mohan Malviya Engineering College, Gorakhpur-273010, India.